

Supporting Information

Using Boryl-substitution and Improved Suzuki-Miyaura Cross-coupling to Access New Phosphorescent Tellurophenes

Christina A. Braun,^a Nicole Martinek,^a Yuqiao Zhou,^a Michael J. Ferguson^a and Eric Rivard^a

^aDepartment of Chemistry, University of Alberta, 11227 Saskatchewan Drive, Edmonton, Alberta, Canada T6G 2G2

Table of Contents

1.	X-ray structure determinations	S2
2.	Ultraviolet-visible (UV-vis) spectroscopy measurements	S4
3.	Luminescence Images	S5
4.	Lifetime measurements	S6
5.	NMR Spectra	S7
6.	Time dependent density functional theory (TD-DFT) computations for Mes(ⁱ PrO)B-Te-6-B(ⁱ Pr)Mes	S19
7.	References	S23

1. X-ray structure determinations

X-ray Crystallography. Crystals suitable for X-ray diffraction studies were removed from a vial and immediately coated in a thin layer of hydrocarbon oil (Paratone-N). A suitable crystal was then mounted on a glass fiber, and quickly placed in a low temperature stream of nitrogen on an X-ray diffractometer. All data was collected on a Bruker APEX II CCD detector/D8 diffractometer¹ using Cu K α radiation with the crystals cooled to –100 °C. The data was corrected for absorption using Gaussian integration from the indexing of the crystal faces.² Crystal structures were solved using intrinsic phasing SHELXT-2014³ and refined using full-matrix least-squares on F^2 (SHELXL).⁴ The assignment of hydrogen atom positions were based on the sp² or sp³ hybridization geometries of their respective carbon atoms, and were given thermal parameters 20 % greater than those of their parent atoms.

Special refinement conditions for danB-Te-6-Bdan: In the structure of **danB-Te-6-Bdan**, the C11S-C12S distance (carbons of an Et₂O solvent molecule) was constrained by *DFIX* command in *SHELXL* to be 1.4437(11) Å.

Table S1. Crystallographic data for tellurophenes derived from (ⁱPrO)₂B-Te-6-B(OⁱPr)₂.

Compound	catB-Te-6-Bcat	(^t Bucat)B-Te-6-B(^t Bucat)	danB-Te-6-Bdan	Mes(ⁱ PrO)B-Te-6-B(O ⁱ Pr)Mes
formula	C ₂₀ H ₁₆ B ₂ O ₄ Te	C ₂₈ H ₃₂ B ₂ O ₄ Te	C ₄₀ H ₅₄ B ₂ N ₄ O ₃ Te	C ₃₂ H ₄₄ B ₂ O ₂ Te
form. wt. (g/mol)	469.55	581.75	788.09	609.89
crys. dimes. (mm)	0.45×0.04×0.04	0.29×0.16×0.14	0.23×0.23×0.14	0.12×0.09×0.06
Crystal system	Orthorhombic	Triclinic	Monoclinic	Orthorhombic
Space group	<i>P</i> 2 ₁ 2 ₁ 2 ₁ (No. 19)	<i>P</i> 1̄ (No. 2)	<i>P</i> 2 ₁ /c (No. 14)	<i>P</i> nn2 (No. 34)
<i>a</i> (Å)	5.07070(10)	12.0209(3)	15.677(6)	10.0095(3)
<i>b</i> (Å)	17.1292(3)	12.9608(3)	13.588(3)	12.3649(4)
<i>c</i> (Å)	20.6984(4)	18.3885(4)	18.6150(19)	12.5793(4)
α (deg)	-	86.3327(10)	-	-
β (deg)	-	77.7639(9)	91.140(15)	-
γ (deg)	-	69.4855(11)	-	-
<i>V</i> (Å ³)	1797.80(6)	2622.13(11)	3964.8(18)	1556.90(8)
<i>Z</i>	4	4	4	2
ρ _{calcd} (g cm ⁻³)	1.735	1.474	1.320	1.301
μ (mm ⁻¹)	13.26	6.204	6.237	7.720
temperature (°C)	-100	-100	-100	-100
2θ _{max} (deg)	148.13	148.26	149.08	148.15
total data	12381	64505	172797	10692
unique data (R _{int})	3595 (0.0252)	10160 (0.0392)	8062 (0.0391)	3126 (0.0180)
Obs [I > 2σ(I)]	3579	9170	7701	3037
Parameters	246	643	493	171
<i>R</i> ₁ [<i>F</i> _o ² ≥ 2σ(<i>F</i> _o ²)] ^a	0.0203	0.0220	0.0207	0.0158
<i>wR</i> ₂ [all data] ^a	0.0490	0.0597	0.0559	0.0399
max/min Δ <i>r</i> (e Å ⁻³)	1.018/-0.717	0.572/-0.433	0.789/-0.462	0.220/-0.262

^a*R*₁ = Σ||*F*_o| - |*F*_c||/Σ|*F*_o|; *wR*₂ = [Σ*w*(*F*_o² - *F*_c²)²/Σ*w*(*F*_o⁴)]^{1/2}

2. Ultraviolet-visible (UV-vis) spectroscopy measurements

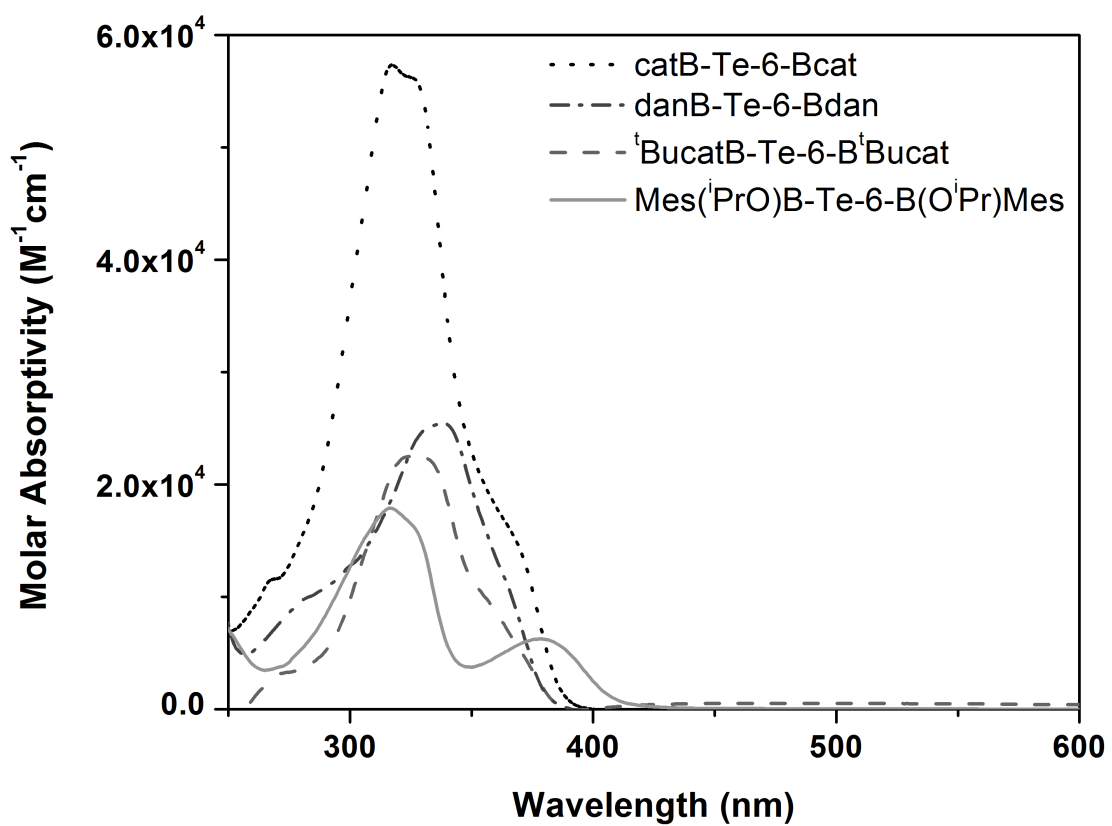


Figure S1. UV-vis absorption spectra recorded in THF, [conc] = 3×10^{-5} M.

3. Luminescence Images

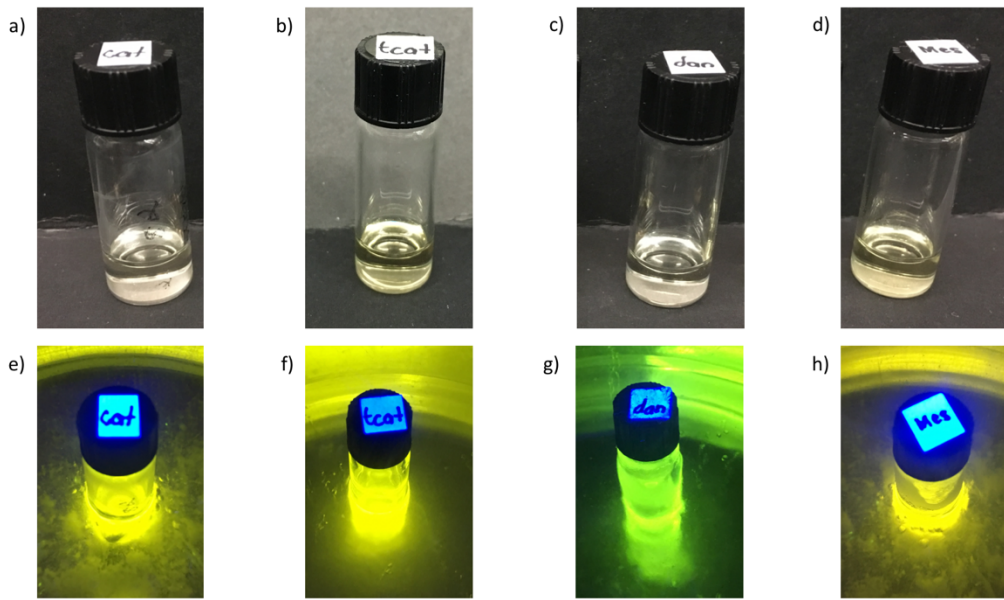


Figure S2. Top: Solutions of a) **catB-Te-6-Bcat**, b) **'BucatB-Te-6-B'tBucat**, c) **danB-Te-6-Bdan** and d) **Mes(*i*PrO)B-Te-6-B(*O**i*Pr)Mes** in 2-methyltetrahydrofuran (0.01 – 0.02 M) at room temperature. Bottom: 2-Methyltetrahydrofuran solutions of e) **catB-Te-6-Bcat**, f) **'BucatB-Te-6-B'tBucat**, g) **danB-Te-6-Bdan** and h) **Mes(*i*PrO)B-Te-6-B(*O**i*Pr)Mes** cooled in an N₂(l) bath and irradiated with a handheld UV lamp (365 nm).

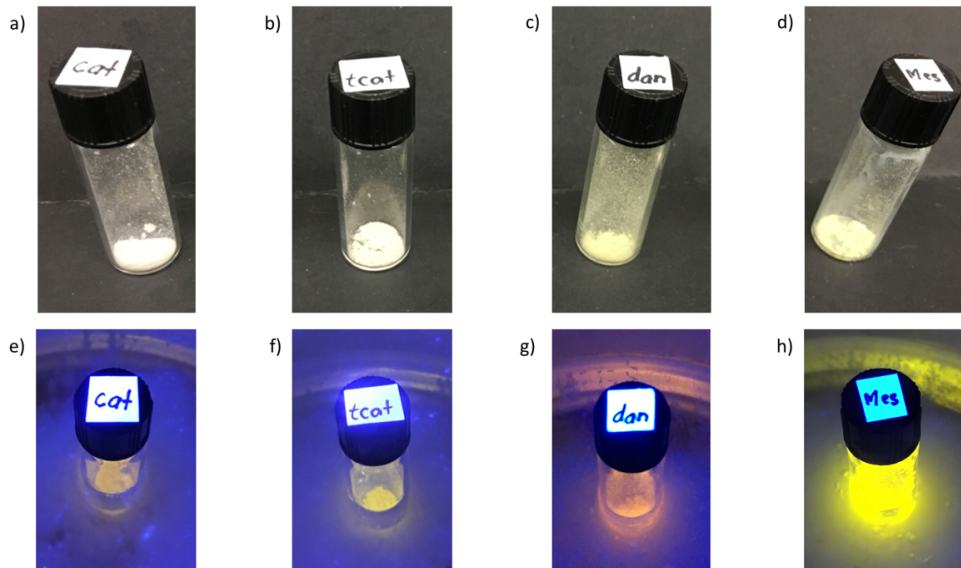


Figure S3. Top: Solid state samples of a) **catB-Te-6-Bcat**, b) **'BucatB-Te-6-B'tBucat**, c) **danB-Te-6-Bdan** and d) **Mes(*i*PrO)B-Te-6-B(*O**i*Pr)Mes** at room temperature. Bottom: Solid state samples of e) **catB-Te-6-Bcat**, f) **'BucatB-Te-6-B'tBucat**, g) **danB-Te-6-Bdan** and h) **Mes(*i*PrO)B-Te-6-B(*O**i*Pr)Mes** cooled in an N₂(l) bath and irradiated with a handheld UV lamp (365 nm).

4. Lifetime measurements

Lifetime measurements were collected on samples sealed in a melting point tube under an N₂ atmosphere. The decay curves were measured using a Horiba PTI QuantaMaster 8075 fluorescence spectrometer equipped with a 75W xenon flash lamp. The resulting decay curve was fitted with the lowest exponential function that gave a suitable reduced chi-square value (χ^2)¹³ and a suitable Durbin Watson parameter.¹⁴⁻¹⁶

Table S2. The photoluminescence decay of **Mes(ⁱPrO)B-Te-6-B(OⁱPr)Mes** powder fit with a biexponential, and the resulting parameters.

Number of components	2
Lifetime of component 1 (τ_1)	81.9517 ± 0.641791 μs
Weight of component 1 (A_1)	0.79
Lifetime of component 2 (τ_2)	160.609 ± 0.378898 μs
Weight of component 2 (A_2)	0.21
Weighted mean lifetime $\left(\frac{\sum A_i \tau_i^2}{\sum A_i \tau_i}\right)$	108.893 μs
χ^2	1.01188
Durbin-Watson parameter	2.03129
Z (run test of the residuals)	-0.00895626

Table S3. The photoluminescence decay of **(^tBucat)B-Te-6-B(^tBucat)** powder fit with a biexponential, and the resulting parameters.

Number of components	2
Lifetime of component 1 (τ_1)	9.1034 ± 0.302457 μs
Weight of component 1 (A_1)	0.61
Lifetime of component 2 (τ_2)	27.9130 ± 0.172553 μs
Weight of component 2 (A_2)	0.39
Weighted mean lifetime $\left(\frac{\sum A_i \tau_i^2}{\sum A_i \tau_i}\right)$	21.5352 μs
χ^2	1.03149
Durbin-Watson parameter	1.86808
Z	-0.0397772

5. NMR Spectra

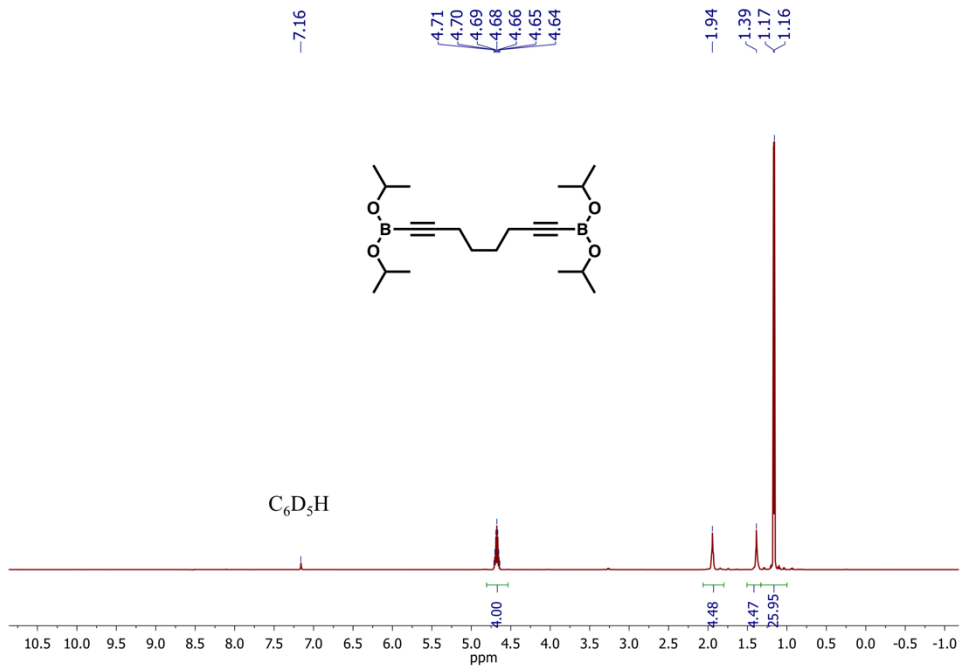


Figure S4. ^1H NMR spectrum of 1,8-bis(diisopropyl-1,3,2-dioxaborolan-2-yl)octa-1,7-diyne in C_6D_6 .

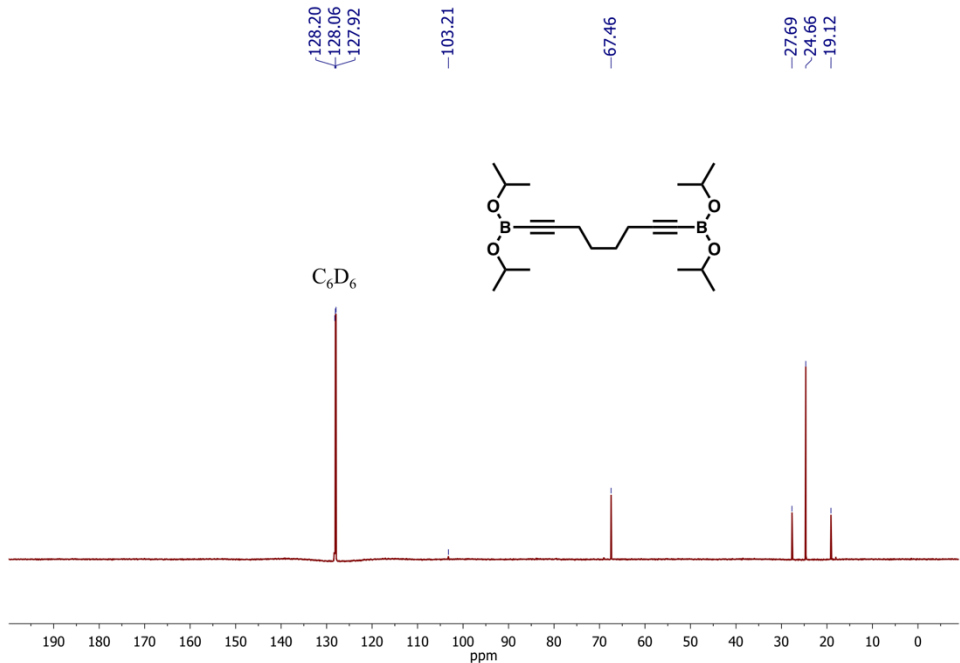


Figure S5. $^{13}\text{C}\{^1\text{H}\}$ NMR spectrum of 1,8-bis(diisopropyl-1,3,2-dioxaborolan-2-yl)octa-1,7-diyne in C_6D_6 .

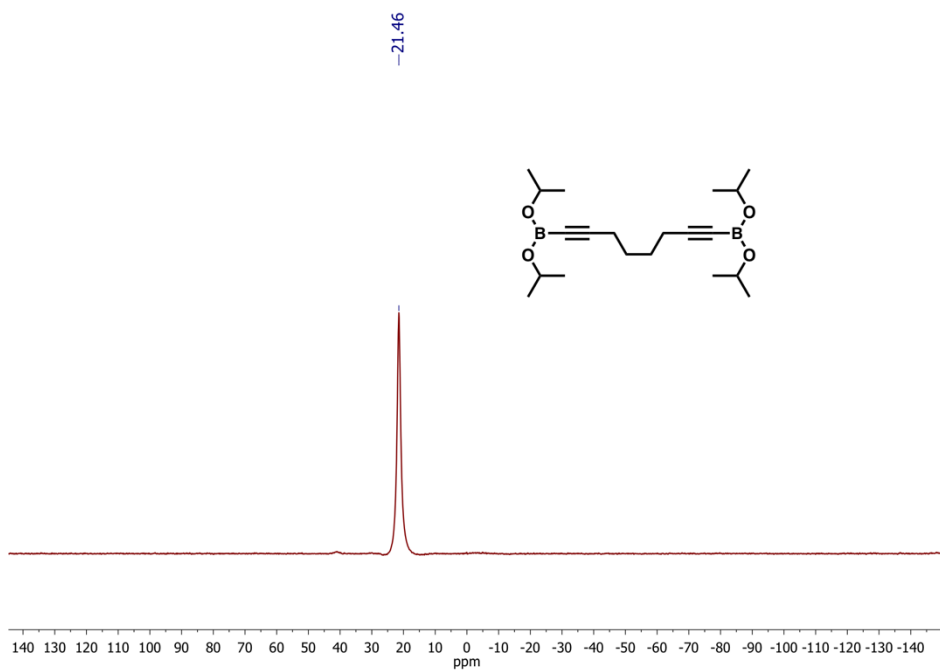


Figure S6. $^{11}\text{B}\{^1\text{H}\}$ NMR spectrum of 1,8-bis(diisopropyl-1,3,2-dioxaborolan-2-yl)octa-1,7-diyne in C_6D_6 .

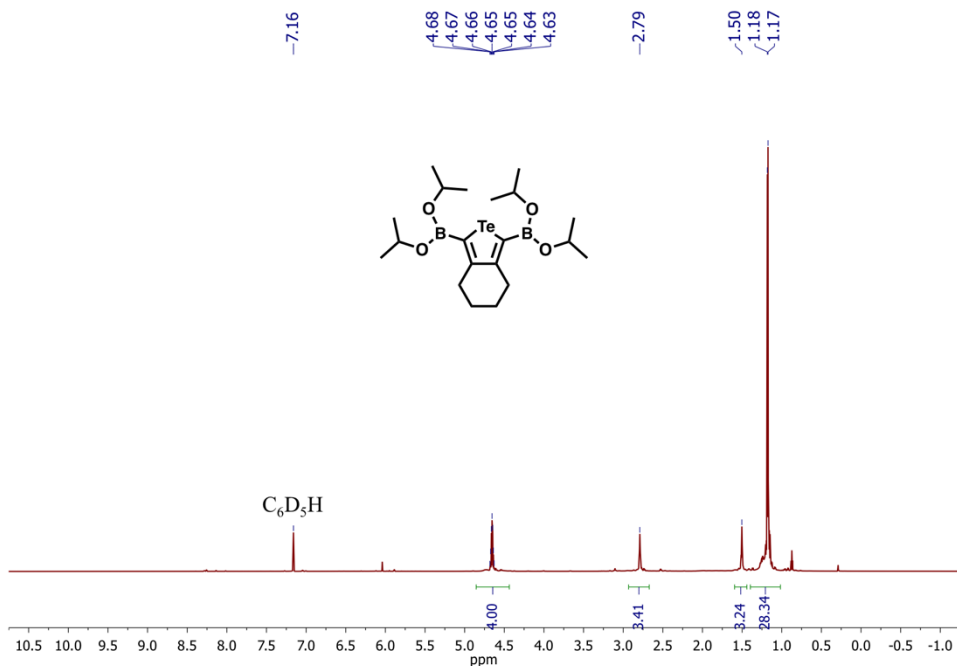


Figure S7. ^1H NMR spectrum of $(\text{iPrO})_2\text{B}-\text{Te}-6-\text{B}(\text{O}\text{iPr})_2$ in C_6D_6 .

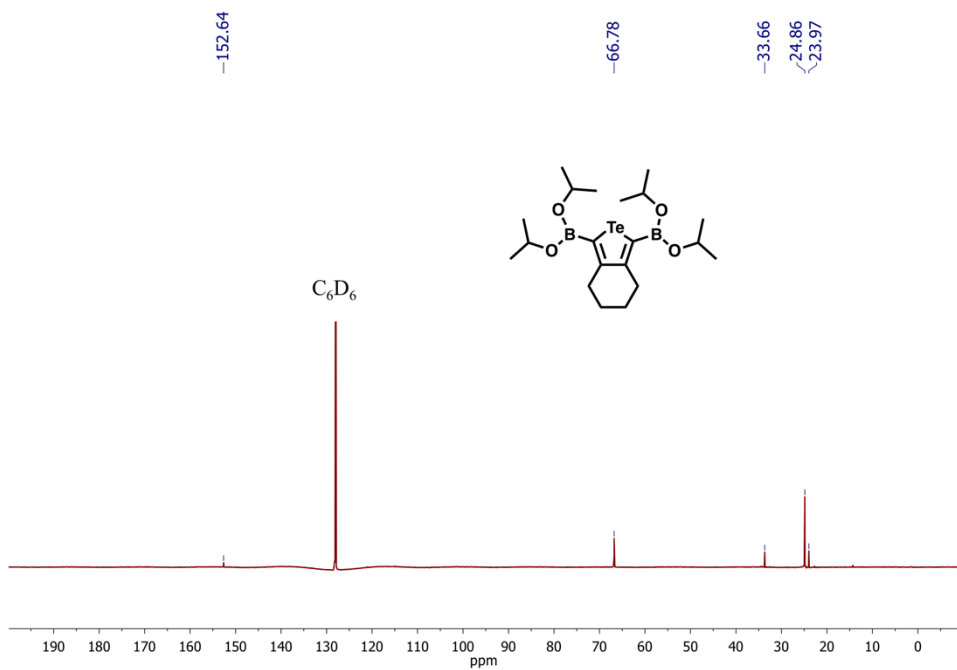


Figure S8. $^{13}\text{C}\{^1\text{H}\}$ NMR spectrum of $(\text{iPrO})_2\text{B-Te-6-B(O}^{\text{i}}\text{Pr})_2$ in C_6D_6 .

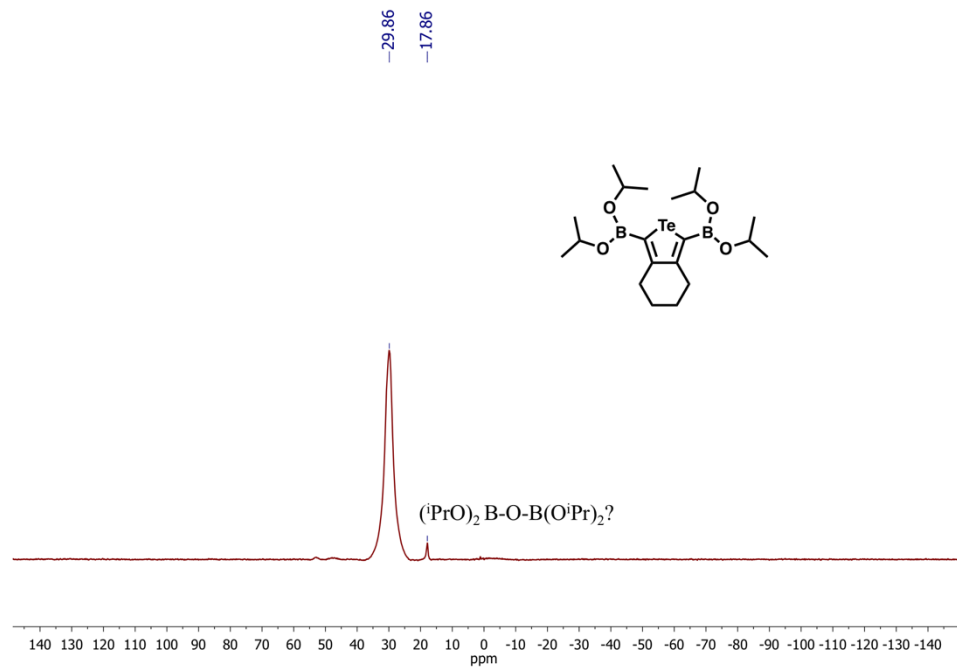


Figure S9. $^{11}\text{B}\{^1\text{H}\}$ NMR spectrum of $(\text{iPrO})_2\text{B-Te-6-B(O}^{\text{i}}\text{Pr})_2$ in C_6D_6 .

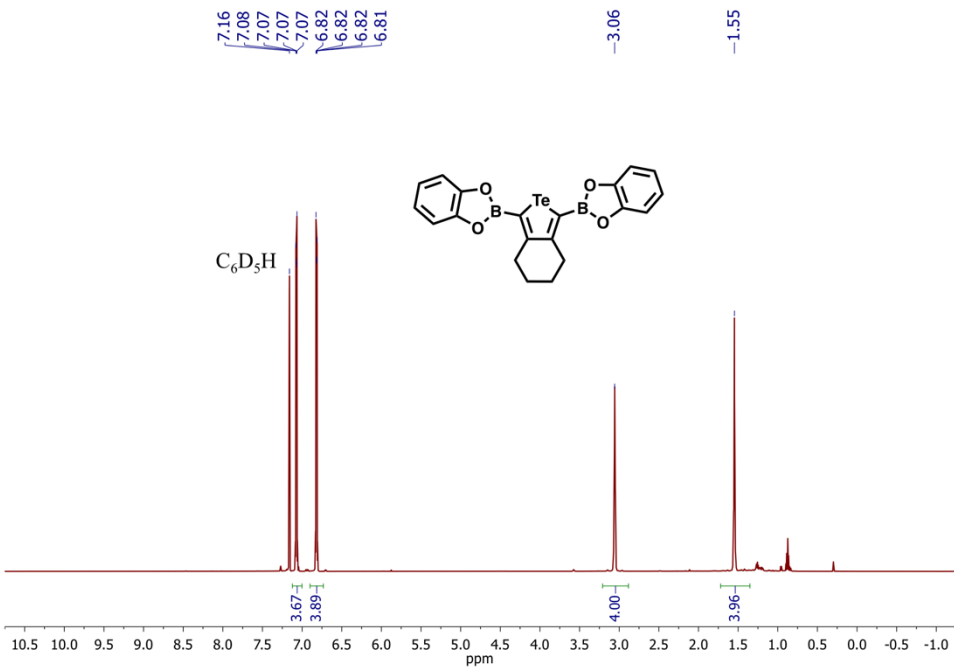


Figure S10. ^1H NMR spectrum of **catB-Te-6-Bcat** in C_6D_6 .

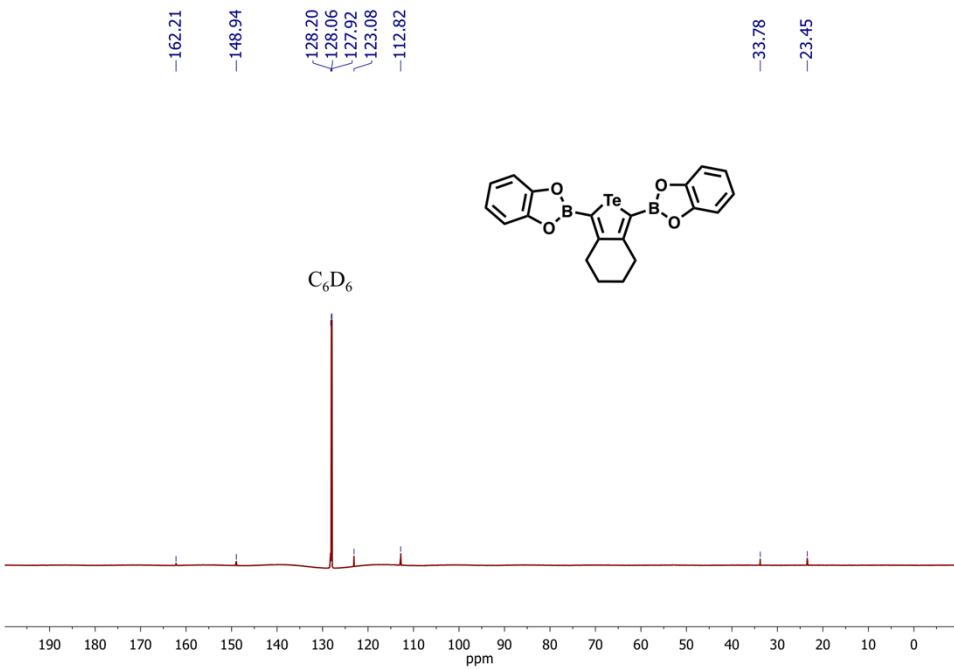


Figure S11. $^{13}\text{C}\{^1\text{H}\}$ NMR spectrum of **catB-Te-6-Bcat** in C_6D_6 .

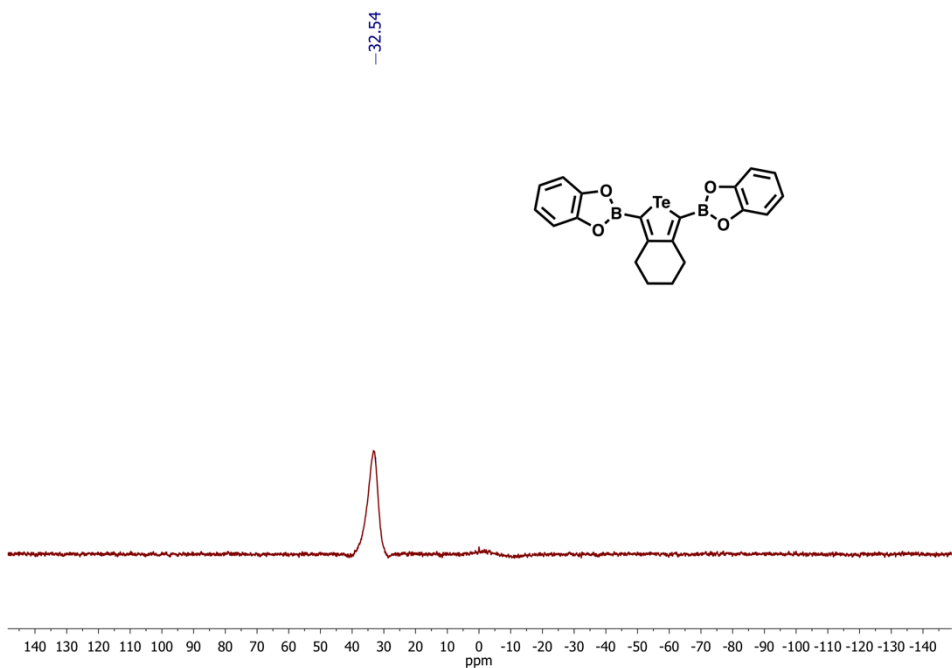


Figure S12. $^{11}\text{B}\{\text{H}\}$ NMR spectrum of **catB-Te-6-Bcat** in C_6D_6 .

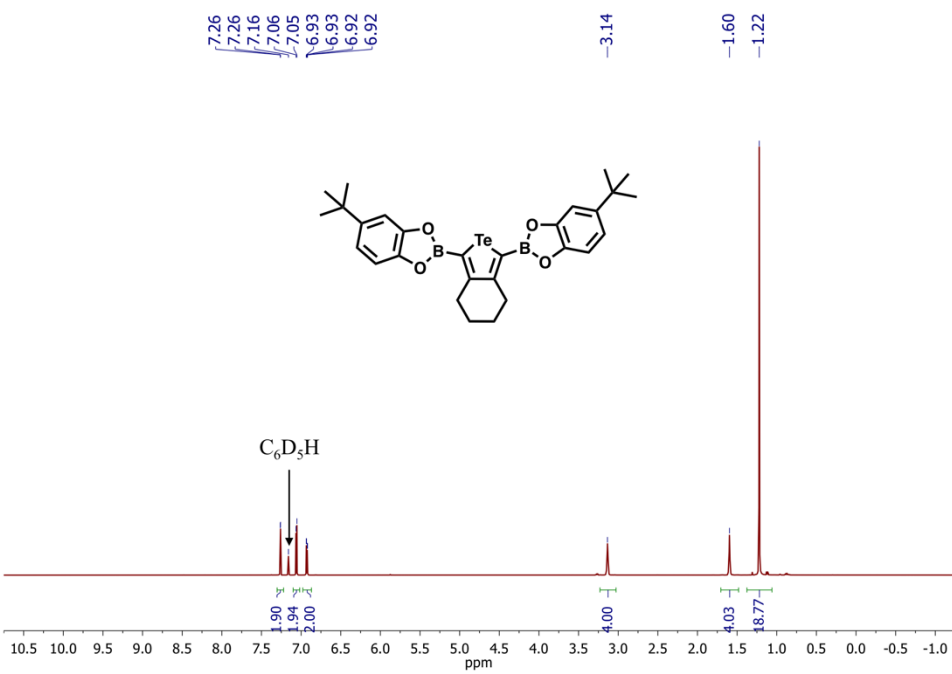


Figure S13. ^1H NMR spectrum of $^t\text{BucatB-Te-6-B}^t\text{Bucat}$ in C_6D_6 .

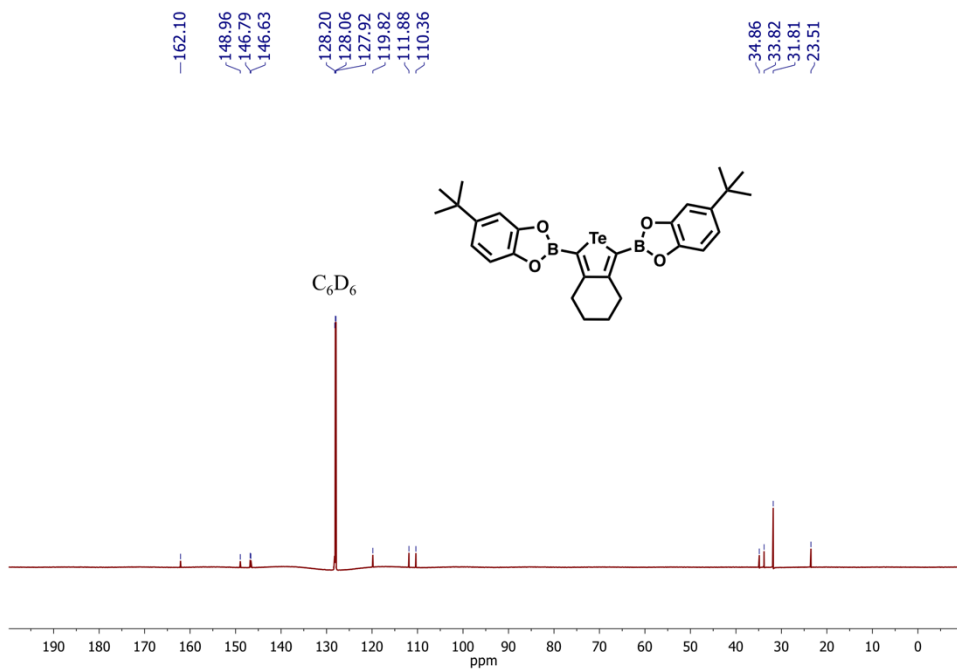


Figure S14. $^{13}\text{C}\{^1\text{H}\}$ NMR spectrum of **tBucatB-Te-6-BtBucat** in C_6D_6 .

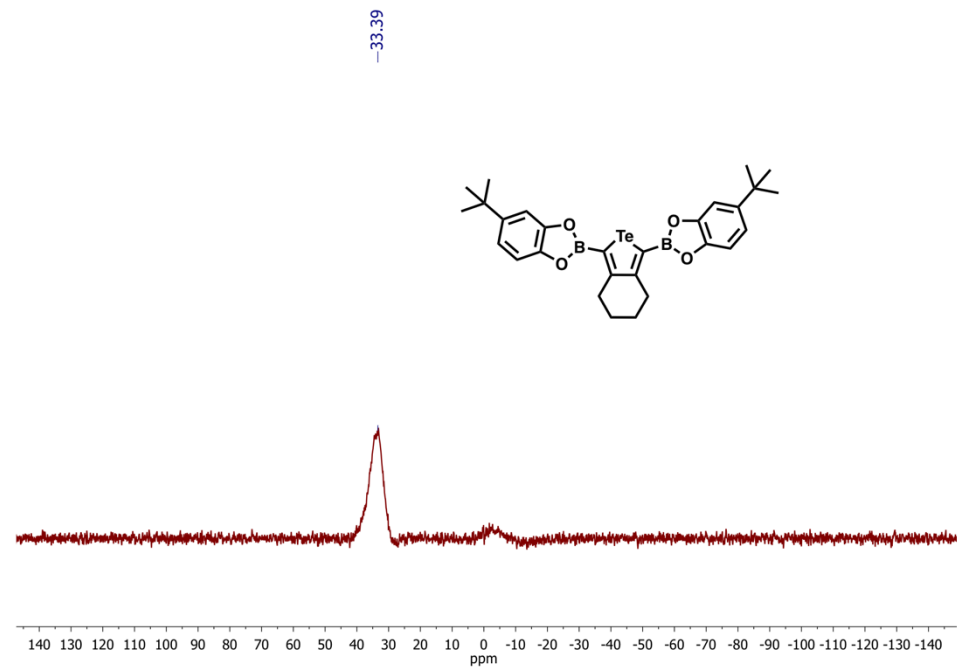


Figure S15. $^{11}\text{B}\{^1\text{H}\}$ NMR spectrum of **tBucatB-Te-6-BtBucat** in C_6D_6 .

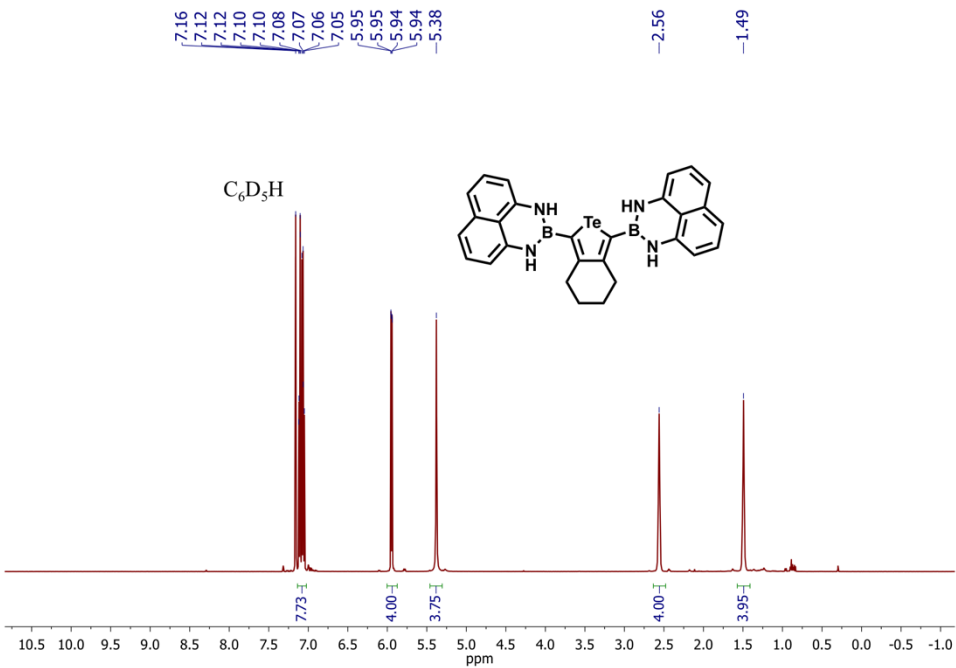


Figure S16. ^1H NMR spectrum of **danB-Te-6-Bdan** in C_6D_6 .

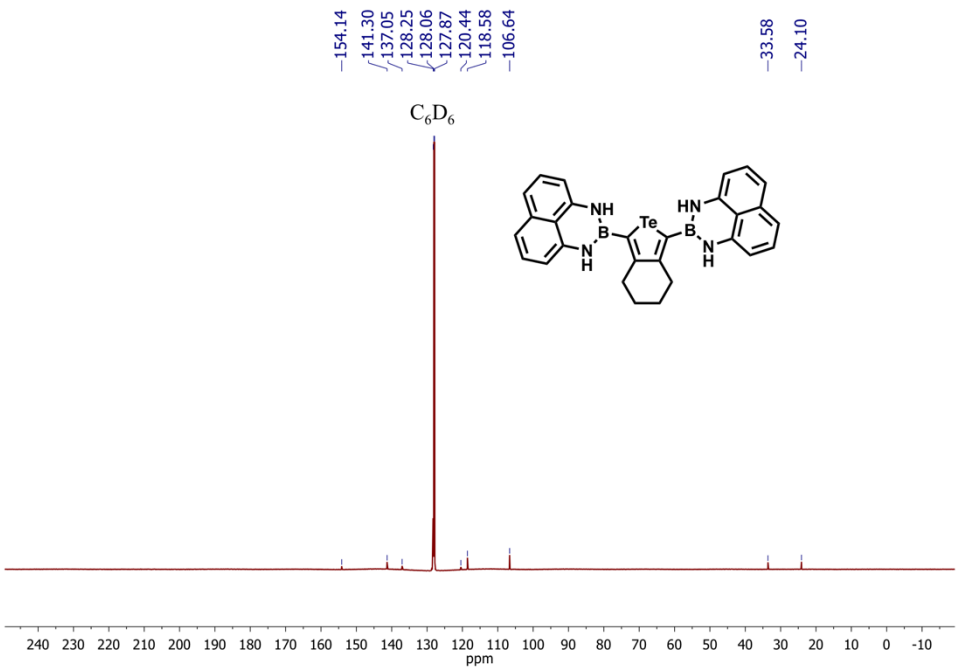


Figure S17. $^{13}\text{C}\{^1\text{H}\}$ NMR spectrum of **danB-Te-6-Bdan** in C_6D_6 .

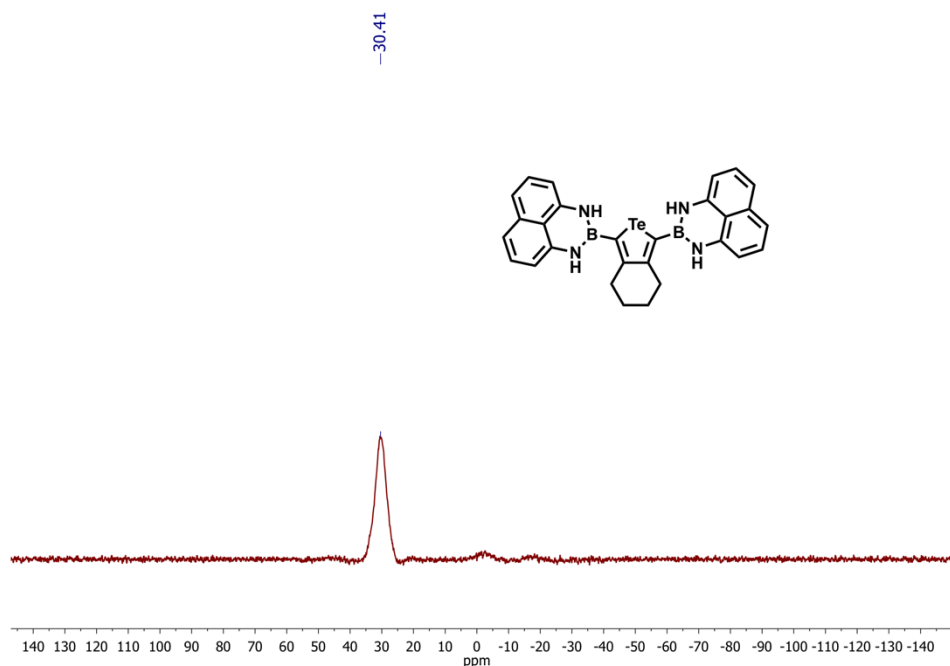


Figure S18. $^{11}\text{B}\{\text{H}\}$ NMR spectrum of **danB-Te-6-Bdan** in C_6D_6 .

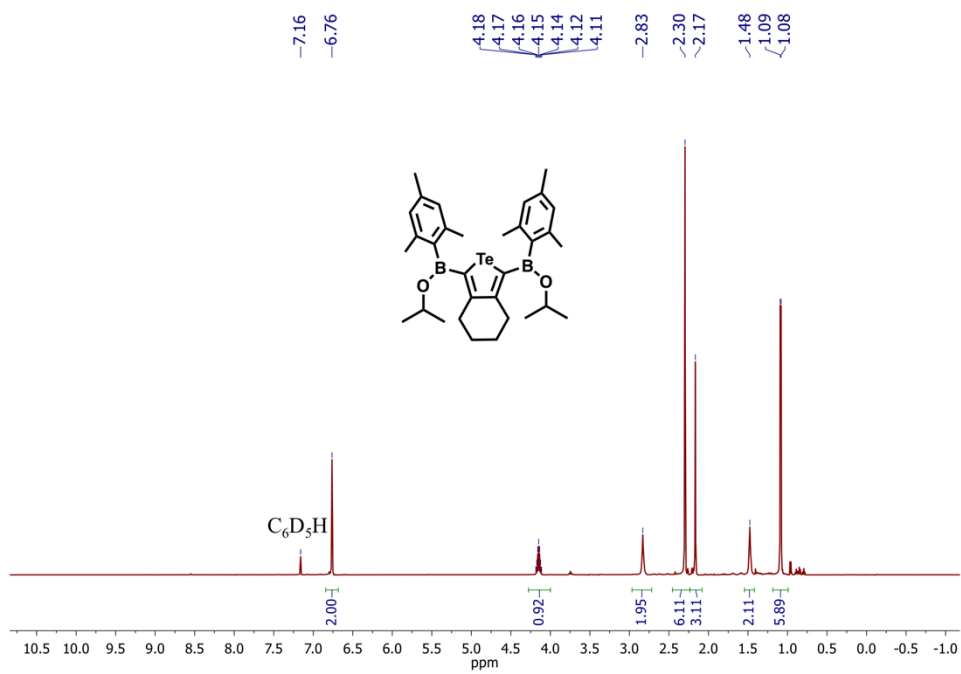


Figure S19. ^1H NMR spectrum of **Mes($i\text{PrO}$)B-Te-6-B($O*Pr*$)Mes** in C_6D_6 .

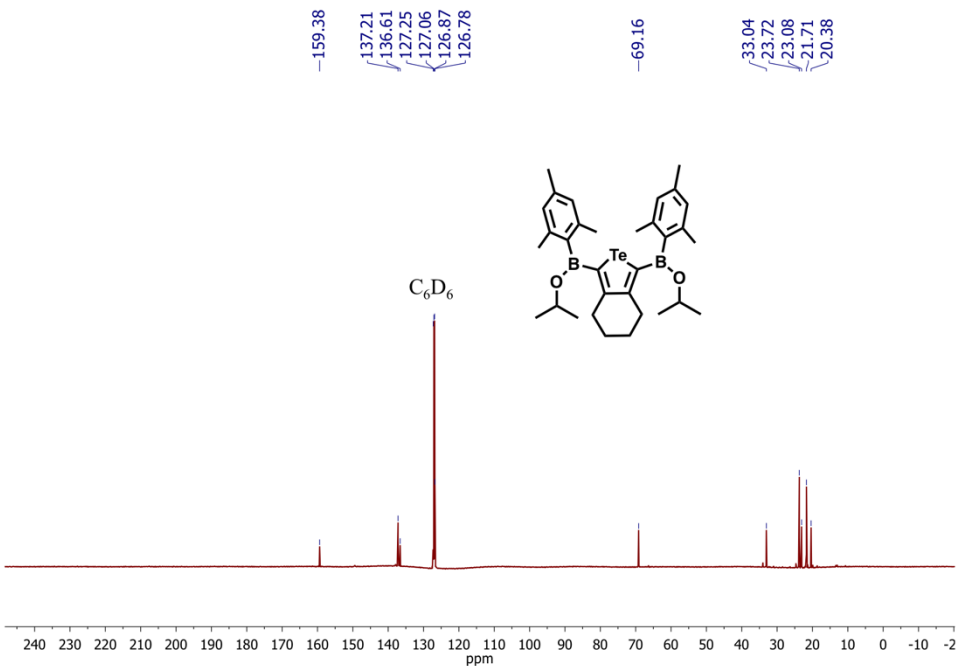


Figure S20. $^{13}\text{C}\{^1\text{H}\}$ NMR spectrum of **Mes(iPrO)B-Te-6-B(O*i*Pr)Mes** in C_6D_6 .

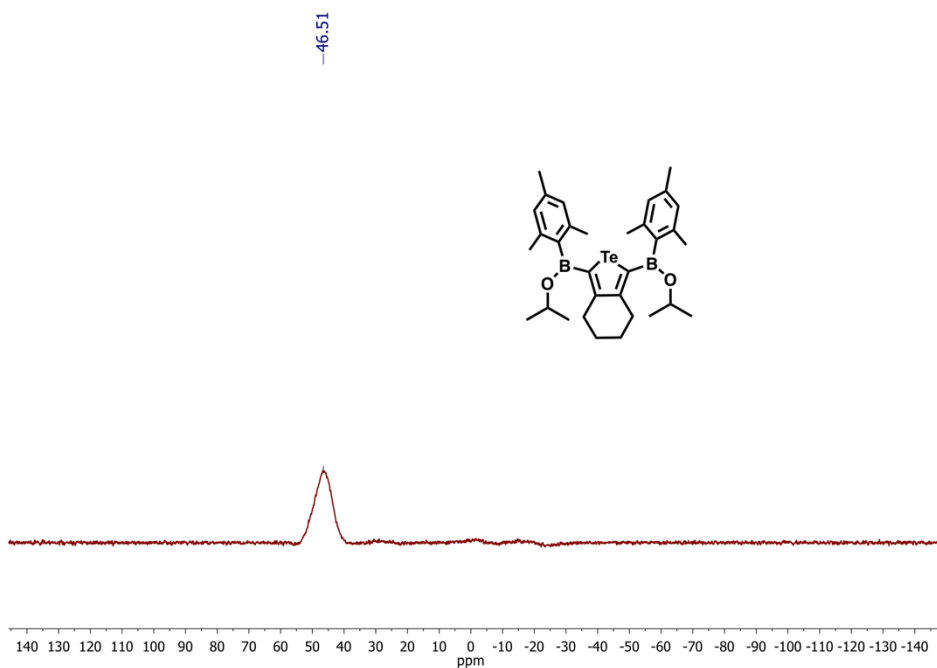


Figure S21. $^{11}\text{B}\{^1\text{H}\}$ NMR spectrum of **Mes(iPrO)B-Te-6-B(O*i*Pr)Mes** in C_6D_6 .

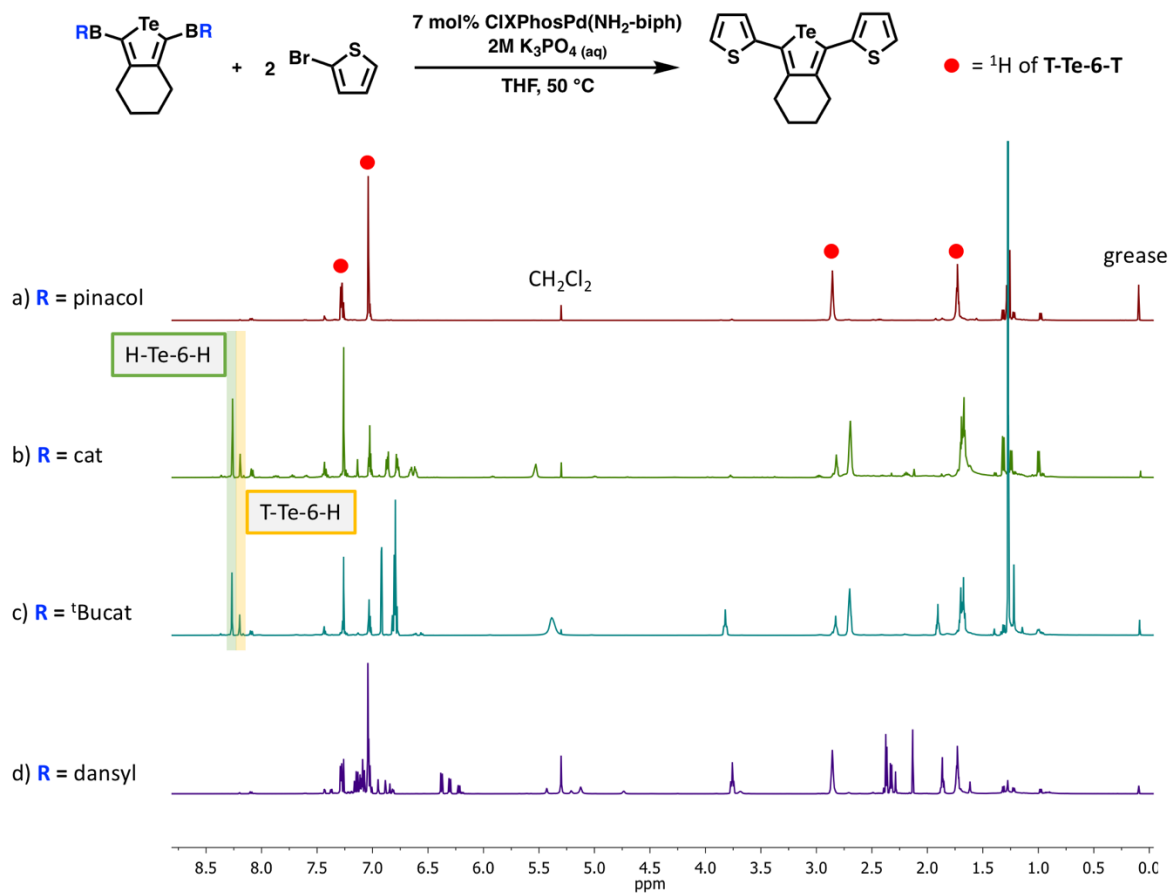


Figure S22. ¹H NMR spectrum (CDCl₃) of the attempted Suzuki-Miyaura cross coupling reactions between borylated tellurophenes and 2 equiv. of 2-bromothiophene. a) coupling with pinB-Te-6-B-pin (16 hrs), b) coupling with catB-Te-6-Bcat (40 hrs), c) coupling with tBucatB-Te-6-BtBucat (40 hrs), d) danB-Te-6-Bdan (16 hrs). All reactions were worked up by diluting with ca. 3 mL of CH₂Cl₂, drying over MgSO₄ and filtering before removing all volatiles. In the above spectra T = thiienyl group.

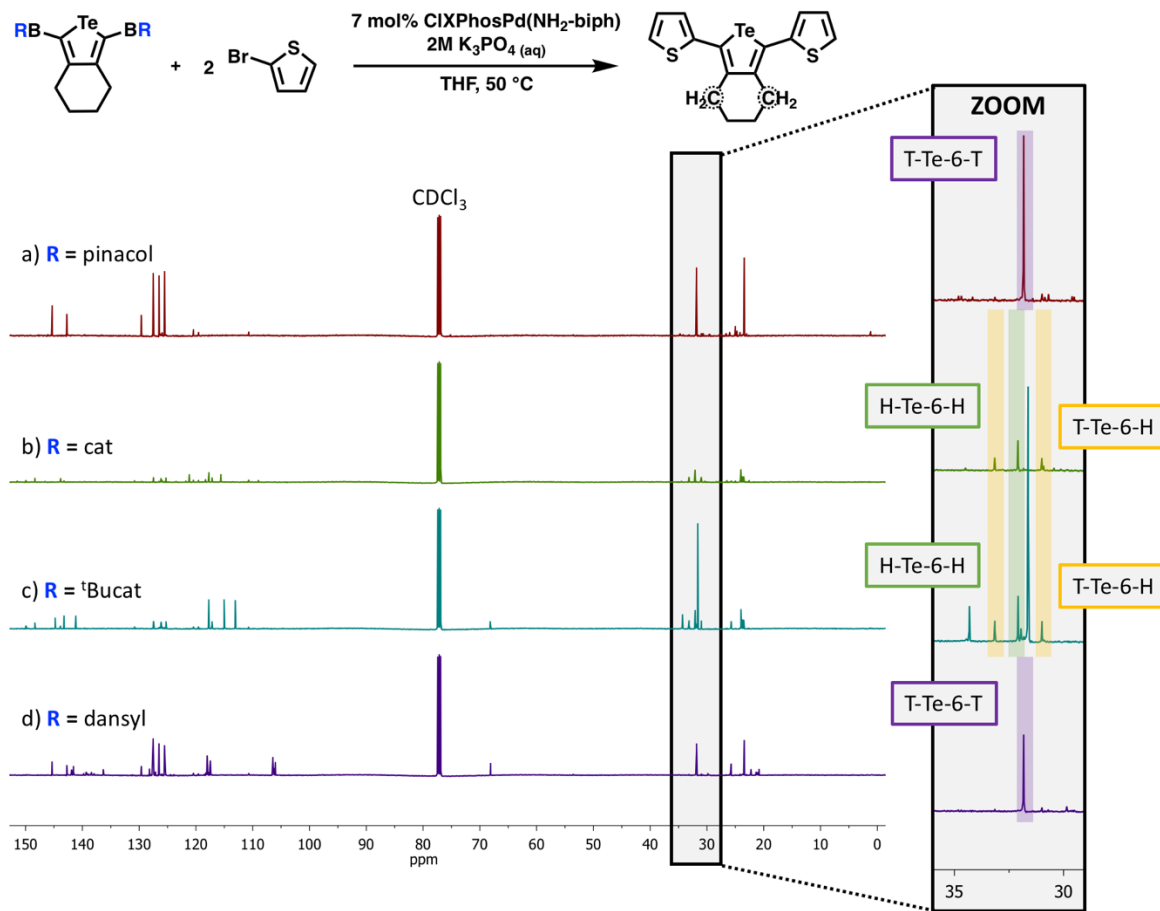


Figure S23. $^{13}\text{C}\{^1\text{H}\}$ NMR spectrum (CDCl₃) of attempted Suzuki-Miyaura cross coupling reactions between borylated tellurophenes and 2-bromothiophene to produce **thienyl-Te-6-thienyl (T-Te-6-T)**. a) coupling with **pinB-Te-6-B-pin** (16 hrs), b) coupling with **catB-Te-6-Bcat** (40 hrs), c) coupling with **¹BucatB-Te-6-B¹Bucat** (40 hrs), d) **danB-Te-6-Bdan** (16 hrs). All reactions were worked up by diluting with *ca.* 3 mL of CH₂Cl₂, drying over MgSO₄ and filtering before removing all volatiles. In the above spectra T = thienyl group.

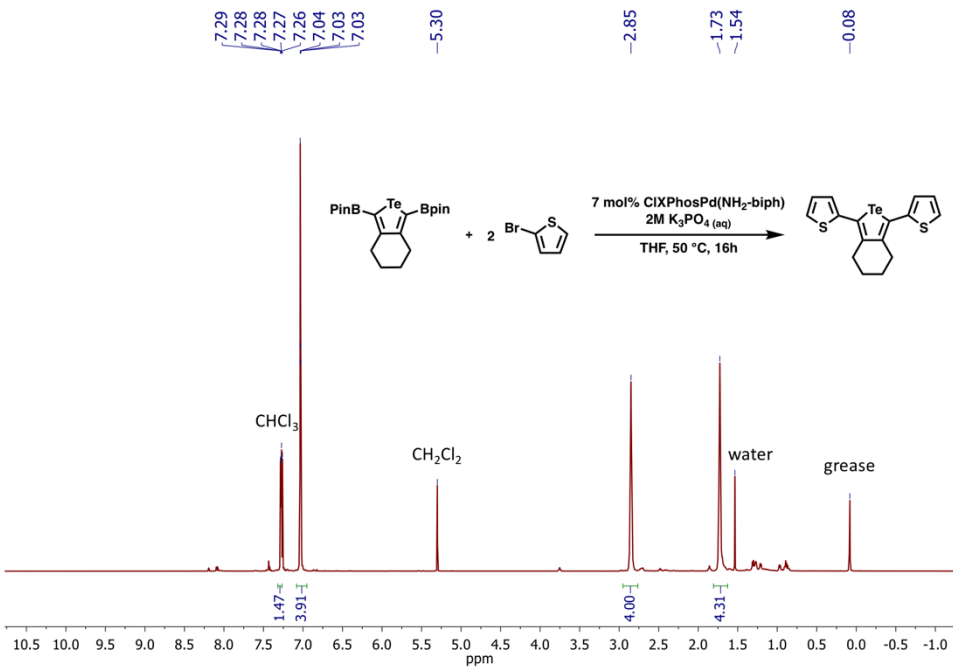


Figure S24. ¹H NMR spectrum of thienyl-Te-6-thienyl (T-Te-6-T) in CDCl₃ produced via the Suzuki-Miyaura cross coupling of pinB-Te-6-Bpin and 2 equiv. 2-bromothiophene.

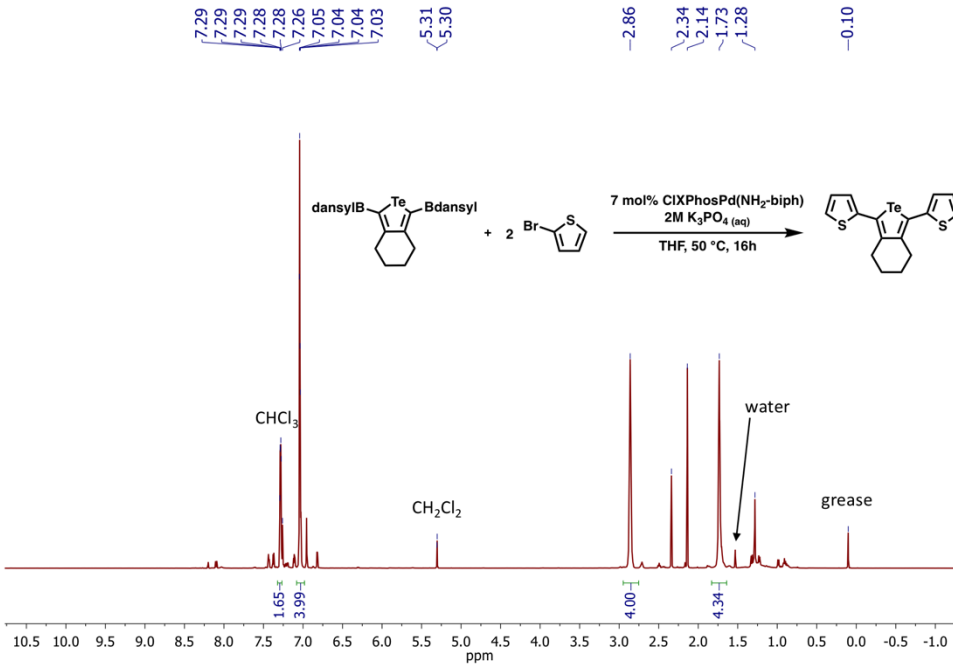


Figure S25. ¹H NMR spectrum of thienyl-Te-6-thienyl (T-Te-6-T) in CDCl₃ produced via the Suzuki-Miyaura cross coupling of danB-Te-6-Bdan and 2 equiv. 2-bromothiophene.

6. Time dependent density functional theory (TD-DFT) computations for Mes(ⁱPrO)B-Te- 6-B(OⁱPr)Mes

All computations have been carried out with the Gaussian16 software package.⁵ Geometry optimizations of the gas-phase structures have been performed using density functional theory (DFT) with the hybrid density functional (B3LYP)^{6,7} in combination with the basis set cc-pVDZ (for C, H, B, O, N)⁸ as well as the basis set cc-pVDZ(-PP) for Te.⁹ The cc-PVDZ-PP basis set uses the corresponding effective core potential (ECP) accounting for 28 electrons. The use of the cc-PVDZ and cc-PVDZ-PP basis sets will hereafter be referred to as cc-PVDZ(-PP). The basis sets as well as the ECP for the Te atom were obtained from the Basis Set Exchange Library.^{10,11} Initial molecular geometries were taken from the experimentally obtained X-ray structures. Subsequent frequency analysis confirmed all obtained structures to be local minima on the potential energy surface. The optimized geometry of the S₀ ground state was determined at the B3LYP level of theory. The phosphorescence energy was calculated by computing the optimized geometry of the lowest lying triplet state (T₁) using UB3LYP (spin-unrestricted B3LYP) with the same basis sets as specified above. Subsequent TD-DFT calculations were used to predict the vertical excitation energies of the first 10 singlet and first ten triplet states using the B3LYP functional as well as the cc-PVDZ(-PP) basis sets starting from the B3LYP optimized gas-phase S₀ geometry. The presented molecule orbitals (MOs) were extracted from the Gaussian16 checkpoint-files and are visualized with VMD.¹²

Table S4. TD-DFT calculated excited states of Mes(ⁱPrO)B-Te-6-B(OⁱPr)Mes at the B3LYP/ccpVDZ(-PP) level of theory.

Excited State	Energy (eV) Oscillator Strength	Wavelength (nm)	Transition
T1	2.4463	506.8	142 – 144
	0.0000		HOMO-1 to LUMO
T2	2.4934	497.3	143 – 144
	0.0000		HOMO to LUMO
S1	3.4273	361.8	143 – 144
	0.0577		HOMO to LUMO
T3	3.5688	347.4	140 – 146
	0.0000		HOMO-3 to LUMO+2
T4	3.5691	347.4	141 – 146
	0.0000		HOMO-2 to LUMO+2
T5	3.8094	325.5	141 – 144
	0.0000		HOMO-2 to LUMO
T6	3.8548	321.6	140 – 144
	0.0000		HOMO-3 to LUMO
S2	3.8633	320.9	141 – 144
	0.0046		HOMO-2 to LUMO
S3	3.8876	318.9	140 – 144
	0.0001		HOMO-3 to LUMO
T7	3.8956	318.3	143 – 145
	0.0000		HOMO to LUMO+1
S4	3.9338	315.2	142 – 144
	0.3590		HOMO-1 to LUMO
T8	4.0703	304.6	139 – 144
	0.0000		HOMO-4 to LUMO
T9	4.0723	304.5	138 – 144
	0.0000		HOMO-5 to LUMO
S5	4.0831	303.7	139 – 144
	0.0021		HOMO-4 to LUMO
S6	4.0847	303.5	138 – 144
	0.0001		HOMO-5 to LUMO
S7	4.2622	290.9	143 – 145
	0.0000		HOMO to LUMO+1
T10	4.4234	280.3	138 – 146
	0.0000		HOMO-5 to LUMO+2
S8	4.7159	262.9	143 – 146
	0.0030		HOMO to LUMO+2
S9	4.7350	261.9	137 – 144
	0.0000		HOMO-6 to LUMO
S10	4.7407	261.5	142 – 145
	0.0014		HOMO-1 to LUMO+1

Table S5. Coordinates for the optimized structure of **Mes(ⁱPrO)B-Te-6-B(OⁱPr)Mes** in the ground state (S_0).

Atom	Coordinates		
	X	Y	Z
Te	0.403955945	0.230358186	1.22239863
O	1.010759912	4.31293258	-0.324681636
C	0.529998639	1.867729981	-0.074677582
C	0.420632011	1.444619295	-1.396749948
C	0.499526979	2.436957755	-2.550324858
H	1.557191849	2.735907035	-2.674747283
H	-0.026601767	3.361211619	-2.277791663
C	-0.021314303	1.88598964	-3.880947155
H	-1.124260662	1.807856386	-3.852624245
H	0.22468247	2.59158818	-4.691760423
C	1.283045405	5.67920875	0.046763567
H	1.354430814	5.742708715	1.145712911
C	0.13117618	6.554823203	-0.438264913
H	0.320699677	7.611252187	-0.188342742
H	0.016172208	6.471972769	-1.531409094
H	-0.818257833	6.258430898	0.032745539
C	2.615123346	6.076679455	-0.58243871
H	2.87160029	7.115335586	-0.318486723
H	3.426685766	5.420656453	-0.233004804
H	2.560954135	5.999898112	-1.680610975
C	0.722296228	3.493390133	2.122142215
C	-0.512394158	3.712094323	2.788117876
C	-0.536733147	3.880559386	4.176350956
H	-1.497633243	4.047763785	4.673313627
C	0.633253912	3.831976874	4.948022591
C	1.84379949	3.610460657	4.286811458
H	2.769444505	3.561832002	4.868715939
C	1.90600121	3.445954179	2.893928591
C	-1.811774032	3.748083587	2.011531418
H	-2.664624771	3.979166748	2.66687037
H	-2.012182709	2.779725812	1.523495932
H	-1.79056011	4.505660205	1.210733786
C	0.573253754	4.003200042	6.447255392
H	0.093806599	4.957465489	6.723492638
H	1.577325155	3.987669556	6.896776545
H	-0.018201251	3.199569095	6.918463621

C	3.256283034	3.242607023	2.238499104
H	3.987384149	2.826437455	2.948386642
H	3.669827216	4.198274796	1.870443524
H	3.198620929	2.559937111	1.3765864
B	0.762562857	3.28128154	0.543037014
O	-0.310768407	-3.03775271	-1.647741152
C	0.202539443	-0.838175614	-0.565602144
C	0.253023512	0.029315383	-1.653613992
C	0.111095034	-0.487315972	-3.08002328
H	-0.953829179	-0.731479774	-3.252728368
H	0.64143957	-1.443385946	-3.180002688
C	0.573288576	0.506260303	-4.149873978
H	1.676980337	0.578768091	-4.147687328
H	0.283136648	0.133895949	-5.146347016
C	-0.577094538	-4.449003544	-1.775267512
H	-0.597047605	-4.900657842	-0.769072673
C	0.54291266	-5.084158717	-2.594363229
H	0.356211806	-6.161889876	-2.728753644
H	0.606876645	-4.616115012	-3.590303994
H	1.516077855	-4.96686308	-2.094047901
C	-1.940813694	-4.607681413	-2.441151515
H	-2.193573342	-5.674391571	-2.552953275
H	-2.72922313	-4.126391479	-1.842925507
H	-1.937904599	-4.14404551	-3.441074156
C	0.10006184	-3.141697508	0.913942291
C	1.362876729	-3.57265429	1.399112633
C	1.451286287	-4.22465302	2.633310897
H	2.433092875	-4.549636457	2.99205843
C	0.319518105	-4.464504247	3.425951585
C	-0.918930322	-4.032408239	2.945089103
H	-1.815600634	-4.202448539	3.549129593
C	-1.045413001	-3.382780299	1.706929265
C	2.623765962	-3.318158834	0.600263324
H	3.504571642	-3.760214914	1.089130106
H	2.80932648	-2.237743606	0.480558342
H	2.558157898	-3.740697655	-0.416007179
C	0.448766138	-5.158333649	4.761059105
H	0.932396537	-6.144169592	4.656043561
H	-0.532780708	-5.312793546	5.233476051
H	1.068791962	-4.570323583	5.459264705

C	-2.42332159	-2.970936927	1.231585348
H	-3.116427214	-2.841515231	2.07686689
H	-2.862094015	-3.73620987	0.567039884
H	-2.400488881	-2.025413325	0.667918405
B	-0.01289173	-2.381028409	-0.482055096

7. References

1. H. Hope, *Prog. Inorg. Chem.*, 1994, **41**, 1.
2. R. H. Blessing, *Acta Crystallogr.*, 1995, **A51**, 33.
3. G. M. Sheldrick, *Acta Crystallogr.*, 2015, **A71**, 3.
4. G. M. Sheldrick, *Acta Crystallogr.*, 2015, **C71**, 3.
5. Gaussian 16, Revision A.03, M. J. Frisch, G. W. Trucks, H. B. Schlegel, G. E. Scuseria, M. A. Robb, J. R. Cheeseman, G. Scalmani, V. Barone, G. A. Petersson, H. Nakatsuji, X. Li, M. Caricato, A. V. Marenich, J. Bloino, B. G. Janesko, R. Gomperts, B. Mennucci, H. P. Hratchian, J. V. Ortiz, A. F. Izmaylov, J. L. Sonnenberg, D. Williams-Young, F. Ding, F. Lipparini, F. Egidi, J. Goings, B. Peng, A. Petrone, T. Henderson, D. Ranasinghe, V. G. Zakrzewski, J. Gao, N. Rega, G. Zheng, W. Liang, M. Hada, M. Ehara, K. Toyota, R. Fukuda, J. Hasegawa, M. Ishida, T. Nakajima, Y. Honda, O. Kitao, H. Nakai, T. Vreven, K. Throssell, J. A. Montgomery, Jr., J. E. Peralta, F. Ogliaro, M. J. Bearpark, J. J. Heyd, E. N. Brothers, K. N. Kudin, V. N. Staroverov, T. A. Keith, R. Kobayashi, J. Normand, K. Raghavachari, A. P. Rendell, J. C. Burant, S. S. Iyengar, J. Tomasi, M. Cossi, J. M. Millam, M. Klene, C. Adamo, R. Cammi, J. W. Ochterski, R. L. Martin, K. Morokuma, O. Farkas, J. B. Foresman and D. J. Fox, Gaussian, Inc., Wallingford CT, 2016.
6. A. D. Becke, *J. Chem. Phys.*, 1993, **98**, 5648.
7. C. Lee, W. Yang, R. G. Parr, *Phys. Rev. B*, 1988, **37**, 785.
8. T. H. Dunning, Jr. *J. Chem. Phys.*, 1989, **90**, 1007.
9. K. A. Peterson, D. Figgen, E. Goll, H. Stoll and M. Dolg, *J. Chem. Phys.*, 2003, **119**, 11113.
10. D. Feller, *J. Comput. Chem.*, 1996, **17**, 1571.
11. K. L. Schuchardt, B. T. Didier, T. Elsethagen, L. Sun, V. Gurumoorthi, J. Chase, J. Li and T. L. Windus, *J. Chem. Inf. Model.*, 2004, **47**, 1045.
12. VMD: W. Humphrey, A. Dalke, and K. Schulten, *J. Mol. Graph.*, 1996, **14**, 33.
13. P. R. Bevington, *IBM J. Res. Develop.*, 1969, **13**, 119
14. J. Durbin and G. S. Watson, *Biometrika*, 1950, **37**, 409.
15. J. Durbin and G. S. Watson, *Biometrika*, 1951, **38**, 159.
16. D. V. O'Connor and D. Phillips, *Time Correlated Single Photon Counting*, Academic Press, New York, 1984.